J Mater Sci (2010) 45:1464–1468
DOI 10.1007/s10853-009-4102-7

Preparation of polymorphic ZnO with strong orange luminescence

Gaohui Du · Yongqiang Yang · Tianbao Li · Bingshe Xu

Received: 27 August 2009 / Accepted: 30 November 2009 / Published online: 18 December 2009

Abstract Polymorphic ZnO has been prepared by a solution method at low temperature (40–90 °C) and the product has been characterized by transmission electron microscopy, UV–vis absorption, and photoluminescence spectroscopy. It is found that the morphology and microstructure of ZnO can be tuned by varying the growth temperature and crystallization condition. The as-synthesized product exhibits narrowed band gap and strong orange luminescence at 620 nm, which may arise from the interstitial oxygen ion defect introduced into ZnO in the solution growth process.

Introduction

Semiconductor nanostructures such as nanowires and quantum dots have a variety of optical and electric properties, which are technologically useful for nanoscale devices. Zinc oxide is a semiconductor with a large direct band gap, large exciton binding energy, and possesses unique optical, acoustic, and electronic properties. ZnO is one of the most intensively studied metal oxides for use in solar cells [1], sensors [2], ultraviolet nanolasers [3], blue light-emitting diodes [4], and field-emission devices. The luminescence of ZnO is generally composed of a strong ultraviolet near-band-edge emission at about 3.3 eV at room temperature and a defect-related emission [5]. The recent researches have demonstrated that the properties vary with the microstructure, morphology, alignment, as well as growth method and conditions [6]. Various shapes of ZnO nanostructures [7–9], such as nanowires, nanobelts, nanocables, and nanohelix, have been fabricated to modify their luminescent properties. Some experimental and theoretical studies have also been performed to tune their electronic structures by doping [10, 11]. For example, Qiu et al. reported that the homogeneous substitution of Zn^{2+} with Co^{2+} in ZnO nanorods lead to a pronounced redshift in the band gap [12]. The optical band gap of the ZnO nanowire arrays has been tuned by simply changing zinc salts in the electrodeposition from aqueous solution, and the reason for the band gap variation is not clear yet [13].

Solution methods are of particular interest for the growth of versatile ZnO nanostructures due to low cost, environmentally friendly, and low-temperature growth. Moreover, the crystal morphology can be easily tuned. In this article, we synthesize ZnO polymorphic structures through adjusting the reaction temperature and crystallization condition. The morphology, microstructure, and optical properties of the products have been investigated and the results demonstrate that they are wurtzite ZnO with narrowed band gap and strong orange emission.

Experimental

ZnO product was prepared by a procedure as follows. 17.6 mL of NaOH (5 mol/L) and 17.6 mL of $ZnCl_2$

G. Du (✉)
Zhejiang Key Laboratory for Reactive Chemistry on Solid Surfaces, Institute of Physical Chemistry, Zhejiang Normal University, 321004 Jinhua, China
e-mail: gaohuidu@zjnu.cn

G. Du · Y. Yang · T. Li · B. Xu (✉)
Key Laboratory of Interface Science and Engineering in Advanced Materials of Taiyuan University of Technology, Ministry of Education, 030024 Taiyuan, China
e-mail: xubs@public.ty.sx.cn

Y. Yang · T. Li · B. Xu
College of Materials Science and Engineering, Taiyuan University of Technology, 030024 Taiyuan, China

(0.5 mol/L) aqueous solution were prepared and added into a flask (100 mL) with 20 mL of deionized water. The mixture was subsequently maintained at the desired temperature (40–90 °C) in a water-bath for 3 h under static or stirring condition. After reaction, the solution was allowed to cool to room temperature. The white precipitates were separated using centrifugation, washed with deionized water thrice, and dried at 60 °C.

The as-prepared samples were characterized using scanning electron microscopy (SEM, Hitachi S4800) and transmission electron microscopy (TEM, JEOL 2010). Photoabsorption of the samples was recorded in a wavelength range of 250–700 nm using a UV–vis spectrophotometer (Nicolet Evolution 500). Photoluminescence (PL) measurement was performed at room temperature using a FS 9200 luminescence spectrophotometer ($\lambda_{ex} = 310$ nm, Xe lamp).

Results and discussion

Figure 1a is the SEM image of the ZnO products obtained at 60 °C under stirring condition. The as-grown ZnO shows a flower-like morphology with a size of 1–2 µm; each flower is composed of many ZnO nanorods with a length of 0.5–1 µm and a diameter of about 90 nm. To investigate the effect of the stirring on the growth of ZnO, another experiment was performed at the same condition except keeping the reaction solution static. As shown in Fig. 1b, it is evident that the morphology of the product changed to big spindle-like rods. The lengths of the rods are about 2–3 µm and their diameters are in the range of 0.3–0.6 µm. So, the product is much larger than that obtained under stirring condition. The difference is caused by the stirring that make the internal environment of the solution uniform and the nucleus can simultaneously form and grow under the same condition. The stirring in the solution method is advantageous to the formation of nanoscale product.

To further understand the growth process of ZnO, different reaction temperature has been used. Shown in Fig. 2a, b is the SEM images of the products obtained at 40 and 90 °C under stirring condition. The holistic morphologies are similar with that formed at 60 °C; the diameter of ZnO nanorods increases from about 70 to 110 nm when the growth temperature varies from 40 to 90 °C. When the reaction solution was kept under static condition, the product appears remarkable change in morphology, and their sizes increase enormously (Fig. 3c, d). The product at 90 °C shows straight and uniform ZnO hexagonal prisms with an average diameter of 0.9 µm and a length of about 9 µm. All the products are confirmed to be pure wurtzite ZnO (space group p63mc; JCPDS Card No. 36-1451) by X-ray diffraction technique.

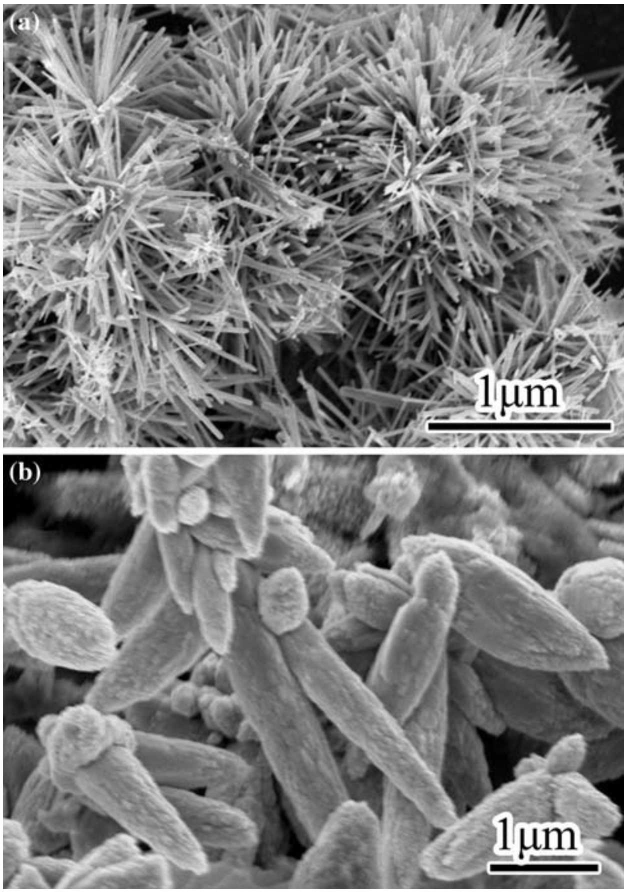

Fig. 1 SEM images of the flower-like ZnO prepared at 60 °C under stirring (**a**) and static condition (**b**)

The morphology and microstructure of ZnO products have been further examined using TEM. ZnO nanorods from 60 and 90 °C under stirring condition are similar in flower-like shape (Fig. 3a, b). A difference between them is the shape of their ends: ZnO nanorods produced at 60 °C have tapering ends, while ZnO nanorods obtained at 90 °C have flat ends. Figure 3c is a TEM image of ZnO rods obtained at 40 °C without stirring. The diameter is about 150–200 nm, which is larger than that of the ZnO nanorods prepared at 60 and 90 °C under stirring. Therefore, the diameters of ZnO nanorods increase with higher growth temperature and static crystallization condition. A selected-area electron diffraction (SAED) taken from a single nanorod (Fig. 3a) is shown in Fig. 3d, and it demonstrates that ZnO nanorod is single crystalline. The SAED pattern can be indexed as hexagonal wurtzite ZnO.

The optical properties of three ZnO samples have been measured using UV–vis absorption and PL spectroscopy. The absorption spectra of the ZnO products are shown in Fig. 4. It is apparent that the synthesized ZnO possesses strong absorbance in visible region. In addition, their absorbance edge shows a blue shift when the ZnO size

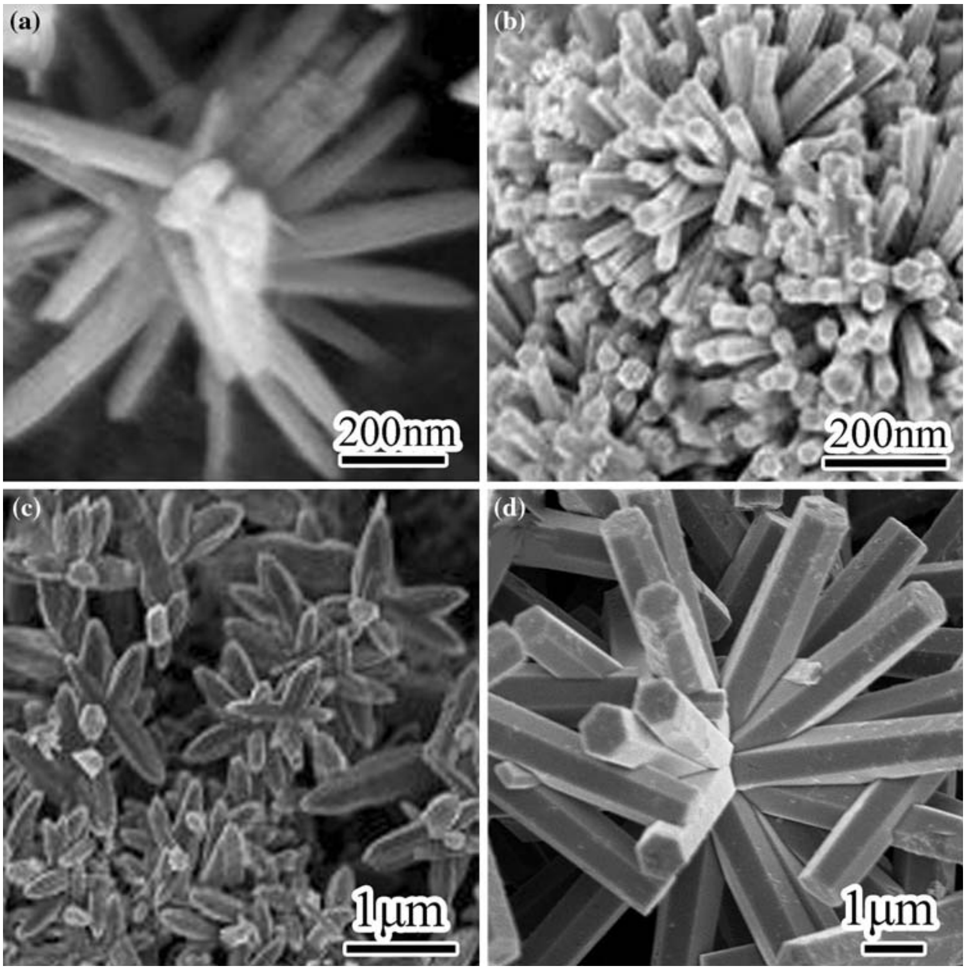

Fig. 2 SEM images of the as-grown ZnO obtained at 40 °C (**a**) and 60 °C (**b**) under stirring condition. (**c**, **d**) ZnO products from 40 and 60 °C under static condition

reduces, indicating their band gaps enlarge with the decrease of the sizes.

The direct band gap energy (E_g) for the ZnO products is estimated by fitting the absorption data to the direct transition equation:

$$(ahv)^2 = A\left(hv - E_g\right)$$

where a is the optical absorption coefficient, hv the photon energy, E_g the direct bandgap, and A a constant [14]. Plotting $(ahv)^2$ as a function of photon energy and extrapolating the linear portion of the curve to the photon energy axis as shown in the *inset* of Fig. 4 give the value of the direct band gap (E_g) to be 3.02, 3.11, and 3.15 eV, respectively. These values are smaller than that of bulk ZnO (3.2 eV) in literature [15]. In general, the absorption edges of nanoscale materials show a blue shift and their band gaps enlarge compared with the bulk due to quantum size effects. The reason of the band gap narrowing in our experiments is not clear; it may originate from the introduction of defects or ion adsorption during the solution growth.

Photoluminescence spectra of the three synthesized ZnO are shown in Fig. 5. The spectra of the ZnO sample are in similar profile and mainly consist of two emission bands: a sharp blue emission band centered at 468 nm (2.64 eV) and a strong, broad orange emission band centered at 620 nm (2.00 eV). The PL is considerably different from the typical observation in ZnO crystals, which usually exhibited a narrow UV peak at 370–390 nm and a broad green emission [16]. The UV near-band-edge emission is not observed in our PL spectra; this absence has also been reported elsewhere [17]. The origin of visible PL in ZnO is still a contentious issue because many kinds of extrinsic and intrinsic lattice defects with different ionization states could be responsible for it [18]. According to previous reports, the blue luminescence at 468 nm may result from the surface defects on the ZnO samples [19]. The orange emission is rarely reported and it arises from optical transitions in the single negatively charged interstitial oxygen ion (O_i^-) inside the grain [20, 21]. There are excess oxygen ions in the precursor aqueous solution. When the aqueous solution is heated, a transition from $\mathrm{Zn(OH)}_4^{2-}$ ions to ZnO

Fig. 3 TEM images of ZnO samples prepared at 60 °C (**a**) and 90 °C (**b**) under stirring condition; **c** TEM images of ZnO sample prepared at 40 °C under static condition. **d** A SAED pattern recorded from an individual ZnO nanorod in (**a**)

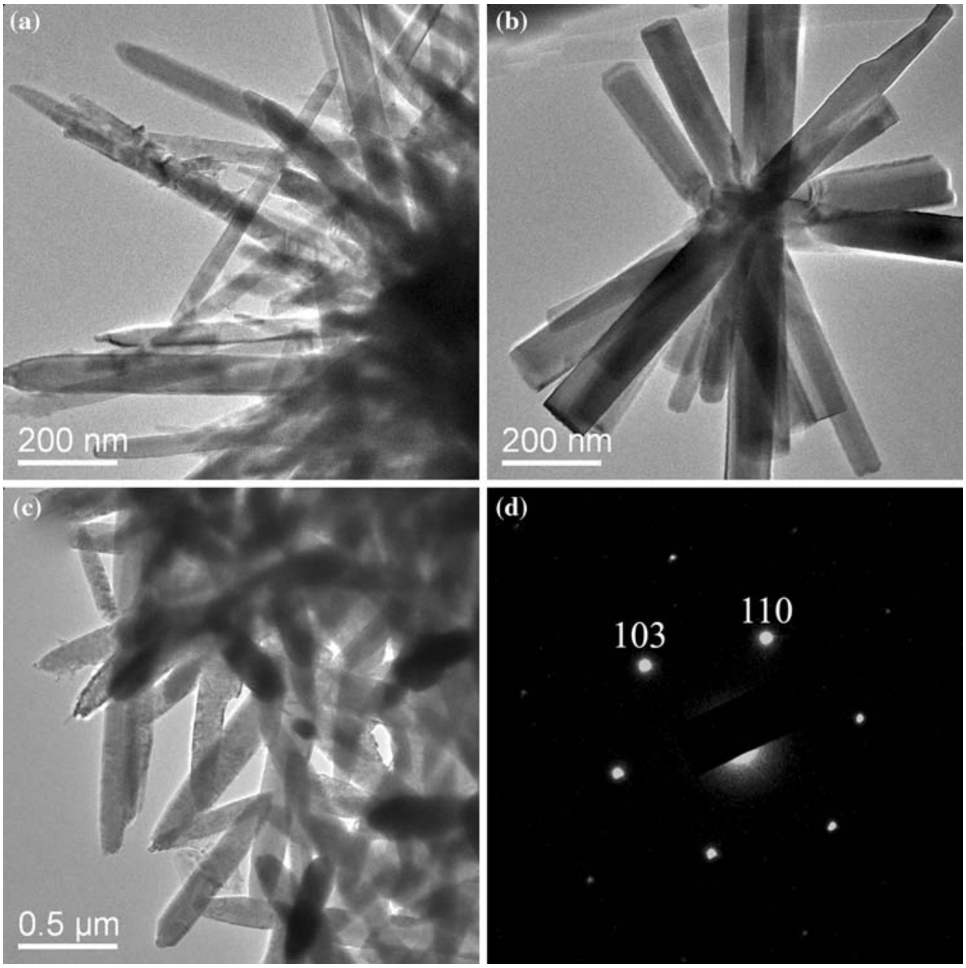

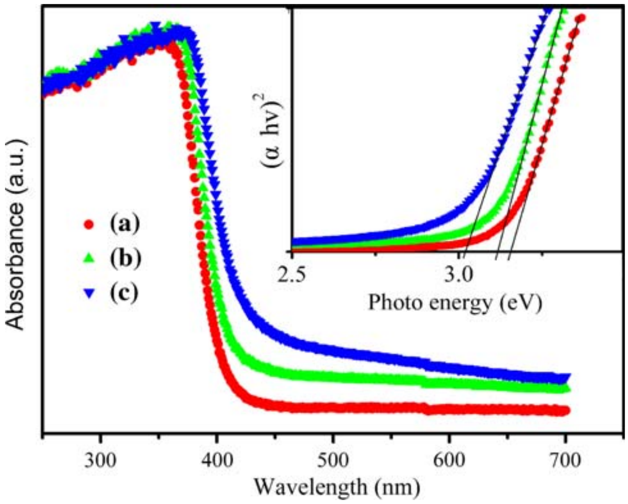

Fig. 4 UV–vis absorption spectra of ZnO samples synthesized at: *a* 60 °C under stirring, *b* 90 °C under stirring, *c* 90 °C under static condition. The *inset* shows the plot of $(ah\gamma)^2$ as a function of photon energy for the ZnO samples

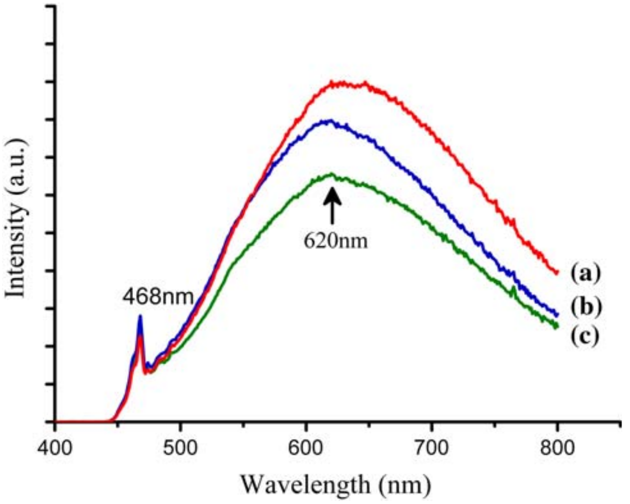

Fig. 5 PL spectra of the ZnO samples synthesized at: *a* 60 °C under stirring, *b* 90 °C under stirring, and *c* 90 °C under static condition

crystals occurs. Some oxygen ions may enter into the interstitial sites of the ZnO crystal lattice and form O_i^-. The orange emission is attributed to the radiative recombination of a delocalized electron close to the conduction band with a deeply trapped hole in O_i^- centers. The sample in Fig. 5a was prepared at 60 °C under stirring and has the smallest size, while that in Fig. 5c has the largest size and better crystallinity in the three samples. It can be seen that the PL intensity in the orange emission increases obviously when the ZnO size decreases. It indicates that the existence of more O_i^- with the decreasing of particle sizes. It is understandable since the crystallization at lower temperature is prone to introduce more defects.

Conclusions

Polymorphic ZnO has been successfully synthesized using a low-temperature solution method without any surfactant or stabilizing agent. The growth temperature and the stirring during crystallization determine the morphology and size of the final product. The UV–vis absorption spectra reveal that the synthesized ZnO samples have narrowed band gaps. It is also found that there exist a blue emission at 468 nm and a strong orange emission at 620 nm in their PL spectra. The band gap narrowing and strong orange emission performance may be caused by the specific defects (e.g., O_i^-), which are introduced into ZnO product during the low-temperature solution growth.

Acknowledgements This work was supported by Shanxi Province Science Foundation for Youths (2008021029-2), Shanxi Province Foundation for Returnees (2007-39), Ministry of Science and Technology of China (2007DFA50940), and National Science Foundation of China (10904129).

References

1. O'Regan B, Schwarthz DT, Zakeeruddin SM, Grätzel M (2000) Adv Mater 12:1263
2. Lin HM, Tzeng SJ, Hsiau PJ, Tsai WL (1998) Nanostruct Mater 10:465
3. Huang MH, Mao S, Feick H, Yan H, Wu Y, Kind H, Weber E, Russo R, Yang P (2001) Science 292:1987
4. Tsukazaki A, Ohtomo A, Onuma T, Ohtani M, Makino T, Sumiya M, Ohtani K, Chichibu SF, Fuke S, Segawa Y, Ohno H, Koinuma H, Kawasaki M (2005) Nat Mater 4:42
5. Ton-That C, Foley M, Phillips RM (2008) Nanotechnology 19:415606
6. Wang ZG, Zu XT, Yang SZ, Wang LM (2006) J Mater Sci 41:3729. doi:10.1007/s10853-006-7180-9
7. Gao P-X, Ding Y, Wang ZL (2009) Nano Lett 9:137
8. Liu ZW, Yeo SW, Ong CK (2007) J Mater Sci 42:6489. doi: 10.1007/s10853-007-1557-2
9. Du GH, Xu F, Yuan ZY, Van Tendeloo G (2006) Appl Phys Lett 88:243101
10. Nakano Y, Morikawa T, Ohwaki T, Taga Y (2005) Appl Phys Lett 87:052111
11. Kim KJ, Park YR (2004) J Appl Phys 96:4150
12. Qiu X, Li L, Li G (2006) Appl Phys Lett 88:114103
13. Anthony SP, Lee JI, Kim JK (2007) Appl Phys Lett 90:103107
14. Ziegler E, Heinrich A, Oppermann H, Stover G (1981) Phys Status Solidi A 66:635
15. Pearton SJ, Norton DP, Ip K, Heo YW, Steiner T (2005) Prog Mater Sci 50:293
16. Ahsanulhaq Q, Kim SH, Kim JH, Hahn YB (2008) Mater Res Bull 43:3483
17. Qian HS, Yu SH, Gong JY, Luo LB, Wen LL (2005) Cryst Growth Des 5:935
18. Tam KH, Cheung CK, Leung YH, Djurisic AB, Ling CC, Beling CD, Fung S, Kwok WM, Chan WK, Phillips DL, Ding L, Ge WK (2006) J Phys Chem B 110:20865
19. Wang J, Gao L (2004) J Cryst Growth 262:290
20. Liu M, Kitai AH, Mascher P (1992) J Lumin 54:35
21. Wu XL, Siu GG, Fu CL, Ong HC (2001) Appl Phys Lett 78:2285